March, 2008

In vivo ultrasonic attenuation slope estimates for detecting cervical ripening in rats: Preliminary results

Timothy A. Bigelow, *University of North Dakota*
Barbara L. McFarlin, *University of Illinois at Chicago*
William D. O'Brien, Jr., *University of Illinois at Urbana-Champaign*
Michael L. Oelze, *University of Illinois at Urbana-Champaign*

In vivo ultrasonic attenuation slope estimates for detecting cervical ripening in rats: Preliminary results

Timothy A. Bigelow[a)]
Department of Electrical Engineering, University of North Dakota, Box 7165, Grand Forks, North Dakota 58202

Barbara L. McFarlin
Department of Maternal Child Nursing, University of Illinois at Chicago, M/C 802, Room 858, 845 S. Damen Avenue, Chicago, Illinois 60612

William D. O'Brien, Jr. and Michael L. Oelze
Bioacoustics Research Laboratory, Department of Electrical and Computer Engineering, University of Illinois at Urbana-Champaign, 405 N. Mathews, Urbana, Illinois 61801

(Received 11 September 2007; revised 10 December 2007; accepted 11 December 2007)

To effectively postpone preterm birth, cervical ripening needs to be detected and delayed. As the cervix ripens, the spacing between the collagen fibers increases and fills with water, hyaluronan, decorin, and enzymes suggesting that the ultrasonic attenuation of the cervix should decrease. The decrease in ultrasonic attenuation may be detectable, leading to an effective means of detecting cervical ripening. Herein, the traditional attenuation slope-estimation algorithm based on measuring the downshift in center frequency of the ultrasonic backscattered signal with propagation depth was modified and applied to the cervix of rats. The modified algorithm was verified using computer simulations and an *ex vivo* tissue sample before being evaluated in *in vivo* animal studies. Spherically-focused f/3 transducers with 33-MHz center frequencies and with 9-mm focal lengths were used in both the simulations and experiments. The accuracy was better than 15% in the simulations, and the attenuation slope of the cervix in the *ex vivo* experiment was 2.6 ± 0.6 dB/cm-MHz, which is comparable to 2.5 ± 0.4 dB/cm-MHz measured using a through-transmission insertion loss technique. For the *in vivo* experiments, a statistically significant effect of ultrasonic attenuation with gestational age was not observed. The large variances in the *in vivo* results were most likely due to the natural variation in attenuation for biological tissue between animals.
 [DOI: 10.1121/1.2832317]

PACS number(s): 43.80.Vj, 43.80.Ev, 43.80.Qf [CCC] Pages: 1794–1800

I. INTRODUCTION

Premature delivery is the leading cause of infant mortality in the United States (Callaghan *et al.*, 2006). Among the infant survivors, 23% suffer a major neurological disability (Wilson-Costello *et al.*, 2007), and it is estimated that just the initial in-hospital care after birth costs $10 billion annually (St. John *et al.*, 2000). In the United States, there has been a 20% increase in the preterm birth rate from 1990 to 2005, to 12.7% of all births (Hamilton *et al.*, 2006). Therefore, there is a medically significant need to develop new methods to prevent premature delivery. Currently, clinicians can only attempt to delay delivery once extensive uterine contractions have been initiated, but these contractions represent the final stage of the process. The cervix prepares for the delivery weeks to months before labor by a process termed preterm cervical ripening without any signs or symptoms currently detectable noninvasively. If preterm cervical ripening could be reliably detected noninvasively before the onset of contractions, then new treatments could potentially be developed to prevent premature delivery.

The role of the cervix during pregnancy before the fetus is mature is to remain strong and resist loading forces that cause it to change and allow delivery of the fetus. The strength of the cervix is due to its anatomic properties (cervical length, thickness) and its tissue properties (collagen and extracellular matrix remodeling) (House and Socrate, 2006). The loading forces are: (1) passive, the enlarged size and weight of the uterus; and (2) active, the forces of the uterine contractions (House and Socrate, 2006). Parturition involves orderly and biologically timed events of the uterus and cervix (Leppert, 1995; Mahendroo *et al.*, 1999; Straach *et al.*, 2005). As the cervix prepares for labor and birth, it first softens early in pregnancy while preserving its ability to maintain the fetus within the uterus and then undergoes a process of remodeling where the collagen concentration decreases and collagen fibrils become disorganized (cervical ripening). Once the cervix softens and then ripens, the forces allow the anatomic changes of cervical thinning, shortening, and finally dilation.

Due to the change in water concentration and tissue morphology (Clark *et al.*, 2006; Feltovich *et al.*, 2005; Leppert *et al.*, 2000), it has been hypothesized that the ultrasonic attenuation of the cervix should drastically decrease during

a)Electronic mail: timothybigelow@mail.und.nodak.edu

cervical ripening. This hypothesis recently received some additional support when the through-transmission insertion loss of *ex vivo* cervical samples from rats at varying gestational ages, 15 to 21 days, was observed to decrease with increasing gestational age (McFarlin *et al.*, 2006). Before the hypothesis can be validated, however, the observations need to be reproduced *in vivo*. Therefore, an algorithm for determining the attenuation from backscattered ultrasonic echoes needs to be implemented and validated for the cervix.

Over the years many algorithms have been proposed for making *in vivo* estimates of the attenuation from backscattered ultrasonic signals. The most common algorithms are based on assuming that the backscattered signals have a Gaussian power spectrum and that the ultrasonic attenuation (loss per distance; e.g., dB/cm) linearly increases with frequency, thus allowing the attenuation to be determined from the downshift in center frequency of the backscattered spectrum (Baldeweck *et al.*, 1994, 1993, 1995; Girault *et al.*, 1998; Hyungsuk and Varghese, 2007; Narayana and Ophir, 1983a, b; Oosterveld *et al.*, 1991). In this study, we followed the traditional approach of using the downshift in center frequency to determine the ultrasonic attenuation slope (attenuation per frequency; e.g., dB/cm-MHz). We implemented the algorithm with the intention of measuring the ultrasonic attenuation slopes of rat cervices *in vivo* using a 33-MHz spherically focused f/3 transducer with a focal length of 9 mm. The algorithm was implemented in the frequency domain, as opposed to using an autoregressive approach, which has been utilized by other investigators (Baldeweck *et al.*, 1994, 1993, 1995; Girault *et al.*, 1998), so that we could compensate for focusing. The accuracy and precision of our implementation of the algorithm was then validated by computer simulations and an experiment performed on an *ex vivo* tissue samples from a rat cervix. The feasibility of extending the work *in vivo* was also demonstrated by preliminary *in vivo* experiments that compared the attenuation slope of pregnant and nonpregnant rats.

II. SUMMARY OF ALGORITHM

When using the downshift in center frequency of the backscattered power spectrum with depth to estimate the *in vivo* attenuation slope of backscattered ultrasonic signals using focused sources, it is necessary to compensate for the effects of focusing (Hyungsuk and Varghese, 2007; Oosterveld *et al.*, 1991). Otherwise, windowed regions in front of the focus will result in an underestimate of the attenuation slope and windowed regions beyond the focus will overestimate the attenuation slope. In our study, we compensated for diffraction or focusing by approximating the field along the beam axis in the focal region by a Gaussian function. Earlier studies have demonstrated that this approximation is sufficiently valid when estimating spectral properties for the purpose of tissue characterization (Bigelow and O'Brien 2004a, b). Also, the width of the window used to gate the echoes was assumed to be small compared to the depth of focus for the transducer so that variations of the field within each gated region could be ignored.

Based on these approximations, the expected backscattered amplitude spectrum from the tissue, $E[|V_{\text{refl}}(f)|]$, would be proportional to

$$E[|V_{\text{refl}}(f)|] \propto f^2|V_{\text{plane}}(f)|e^{-2\alpha_{\text{eff}}z_T}(F_\gamma(f,a_{\text{eff}}))^{1/2}e^{-2\alpha f z_0}e^{-2(z_0^2/w_z^2)}, \quad (1)$$

where $|V_{\text{plane}}(f)|$ is the amplitude spectrum returned from a rigid plane placed at the focal plane in a water bath. For the other variables, α_{eff} is the effective attenuation along the propagation path from the transducer to the focus, z_T is the distance from the aperture plane to the focal plane, $F_\gamma(f,a_{\text{eff}})$ is a form factor that accounts for the frequency dependence of the ultrasonic backscatter at the focus (Insana *et al.*, 1990), z_0 is the distance of the windowed region from the focus, α is the slope of ultrasonic attenuation versus frequency in the focal region that we are attempting to estimate, and w_z is the effective Gaussian depth of focus that results from approximating the field with a Gaussian function. w_z depends linearly on wavelength and is given by $w_z = 6.01\lambda(f\#)^2$ for an ideal spherically focused source, where $f\#$ is the f-number of the source (Bigelow and O'Brien, 2004b). Assuming that the backscattered spectrum can be approximated by $\exp(-(f-\tilde{f}_0)^2/2\tilde{\sigma}_\omega^2)$, an approximation that is valid for soft tissue using standard pulse-echo imaging, Eq. (1) can be written as

$$E[|V_{\text{refl}}(f)|] \propto \exp\left(-\frac{(f-\tilde{f}_0)^2}{2\tilde{\sigma}_\omega^2} - 2\alpha f z_0 - 2\left(\frac{z_0^2}{w_z^2}\right)\right), \quad (2)$$

where $\tilde{f}_0$ and $\tilde{\sigma}_\omega$ are the spectral peak frequency and Gaussian beam width of the backscattered signal from the focus (i.e., $z_0=0$).

Therefore, the impact of focusing can be removed by multiplying the received amplitude spectrum (i.e., magnitude of the Fourier transform of windowed signal) at every window location by $\exp(2z_0^2/w_z^2)$ prior to finding the center frequency of the spectrum of the signal. The ultrasonic attenuation slope of the medium can then be calculated by finding the change in spectral peak frequency, f_{peak}, with depth into the tissue using

$$\alpha = -\frac{1}{2\tilde{\sigma}_\omega^2}\frac{\partial f_{\text{peak}}}{\partial z_0}. \quad (3)$$

III. COMPUTER SIMULATIONS

A. Simulation parameters

The algorithm was first validated using computer simulations. In the simulations, 1000 backscattered echo wave forms were generated by randomly positioning scatterers in a homogeneous attenuating half-space. The scatterers had a Gaussian correlation function [i.e., form factor $F_\gamma(f,a_{\text{eff}}) = \exp(-0.827(ka_{\text{eff}})^2)$] with an a_{eff} of 6 μm and were positioned at a density of 6000/mm^3 ($\sim$5 scatterers/resolution cell). The attenuation slope and sound speed of the half-space were 2 dB/cm-MHz and 1540 m/s, respectively. The correlation length of 6 μm and attenuation slope of

2 dB/cm-MHz correspond to previous values measured for the cervix of pregnant rats (McFarlin *et al.*, 2006). The simulated f/3 source used to obtain the echoes had a center frequency of 33 MHz and a focal length of 9 mm. The reference amplitude spectrum returned from a plane placed at the focal plane for the source was given by

$$|V_{\text{plane}}(f)| \propto \exp\left(-2\left(\frac{f-33\ \text{MHz}}{19.2\ \text{MHz}}\right)^2\right), \tag{4}$$

similar to the source used to determine the ultrasonic attenuation of the rat cervix *in vivo*.

After generating the echoes, the wave forms were combined into 20 sets of 50 wave forms per set. Each wave form was then windowed into five sections with each section having a corresponding length of 0.5 mm along the beam axis. This window length is considerably smaller than the depth of focus (2.9 mm at 33 MHz) for our transducer; therefore, field variations within each window can be neglected. There was 50% overlap between the sections resulting in a total length of 1.5 mm along the beam axis. After windowing, the Fourier transform was obtained for each section, and the amplitude spectra from all 50 wave forms corresponding to the same window location were averaged to obtain an estimate of $E[|V_{\text{refl}}(f)|]$ at that tissue depth. The estimate for $E[|V_{\text{refl}}(f)|]$ was then multiplied by $\exp(2z_0^2/w_z^2)$ before being fit with a Gaussian function to find an estimate for $\tilde{\sigma}_\omega$ and f_{peak}, the new spectral peak frequency, of the spectrum at that window location, z_0. After finding an estimate for $\tilde{\sigma}_\omega$ and f_{peak} for all five locations along the echo, a line was fit to f_{peak} vs z_0 to obtain $\partial f_{\text{peak}}/\partial z_0$ from which α can be calculated using Eq. (3). The accuracy was further improved by using the mean value of $\tilde{\sigma}_\omega$ from the five window locations for $\tilde{\sigma}_\omega$ in the equation.

B. Simulation results

When validating the algorithm, two issues were of concern. First, the algorithm should correctly compensate for the effects of focusing. Second, the algorithm should be stable even if measurement noise reduces the usable bandwidth of the received echoes (i.e., the range of frequencies not corrupted by noise). Focusing compensation was validated by moving the center of the 1.5-mm region used to obtain the estimates from 1.2 mm in front of the focus to 1.2 mm past the focus. Therefore, the total depth used in the simulations was from 1.95 mm in front of the focus to 1.95 mm past the focus for a total length of 3.9 mm. Likewise, the reduction of usable bandwidth was investigated by varying the bandwidth used in the Gaussian fit to find an estimate for $\tilde{\sigma}_\omega$ and f_{peak} from 10 to 50 MHz centered at the approximate location for the spectral peak prior to correcting for focusing.

The results for the simulations are summarized in Fig. 1. The error in the attenuation slope estimate is typically smaller than 15% except for a few window locations. Therefore, reliable estimates should be obtainable even if the usable bandwidth of the signal is significantly reduced by noise. The simulations also demonstrate a trough in the error in the attenuation slope ($\sim -10\%$) at $z_0=0$. This error is of little concern because it is on the same order as other published results that estimated the attenuation slope from the downshift in center frequency (Hyungsuk and Varghese, 2007). The reason for this trough is not clear but may be related to the number of wave forms used (i.e., 50) to obtain the spectrum because other investigators obtained smaller errors when more wave forms (i.e., 256) were used (Baldeweck *et al.*, 1995).

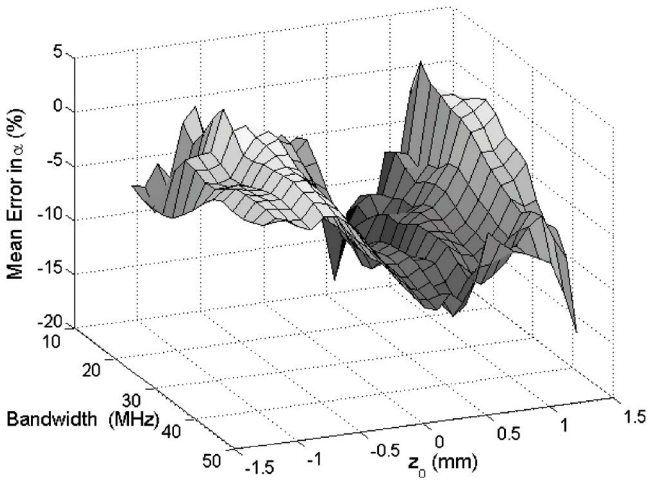

FIG. 1. (Color online) The value of the mean error in the attenuation slope for the simulations vs the usable bandwidth and the location along z_0 of the 1.5-mm section used to obtain the estimates.

Although Fig. 1 indicates that the algorithm is correctly compensating for focusing for the different values of z_0, the performance is easier to evaluate if we restrict our attention to a single frequency range. Figure 2(a) shows the error in the attenuation slope estimate in dB/cm-MHz versus location along the echo using a bandwidth of 35 MHz when performing the Gaussian fit. Figure 2(b) shows the percent error in attenuation slope both with and without focusing compensation. Prior to compensating for focusing, the attenuation slope of regions before the focus is grossly underestimated while the attenuation slope of regions beyond the focus is grossly overestimated. The attenuation slope is underestimated before the focus because $-2\alpha f z_0$ and $-2z_0^2/w_z^2$ have opposite sign (i.e., $z_0<0$) while the attenuation slope is overestimated after the focus because $-2\alpha f z_0$ and $-2z_0^2/w_z^2$ have the same sign (i.e., $z_0>0$). After compensating for focusing, the attenuation slope estimate for all of the regions is approximately the same and within $\sim 10\%$ of the true value for the attenuation.

IV. *EX VIVO* TISSUE EXPERIMENT

Once the algorithm had been validated using computer simulations, the next step was to validate the algorithm using an *ex vivo* tissue sample of a rat cervix. For the *ex vivo* study, we used a custom-fabricated 33-MHz lithium niobate f/3 transducer with a focal length of 9 mm (NIH Transducer Resource Center, University of Southern California, Los Angeles, CA). In this portion of the study, a nonpregnant Sprague-Dawley rat (Harlan, Indianapolis, IN) was euthanized by exposure to CO_2 for 5 min. The experimental protocol was approved by the Institutional Animal Care and Use Committee (IACUC) at the University of Illinois at Urbana-

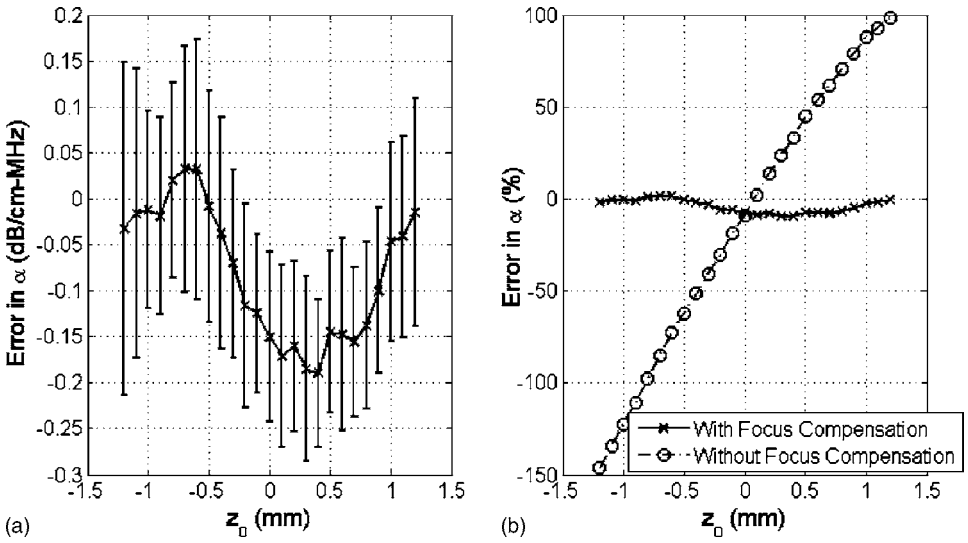

FIG. 2. (a) Difference between estimated and simulated attenuation slope value of 2 dB/cm-MHz plotted vs location along the echo in the simulations using a bandwidth of 35 MHz. The error bars represent one s.d. above and below the mean as calculated using the 20 independent sets of 50 wave forms. (b) Mean error in attenuation vs location along the echo in the simulations both with and without focusing compensation.

Champaign and satisfied all campus and NIH (National Institutes of Health) rules for the human use of laboratory animals. The rat was then weighed prior to necropsy and the cervix was dissected, trimmed, and weighed before being immediately sealed in plastic wrap (Saran Wrap™). A Saran Wrap was used to prevent degradation of the sample over time upon being immersed in degassed water. Because the tissue was surgically removed from the rat, the attenuation slope of the same rat cervix could be estimated by two separate techniques, one of which is the algorithm under evaluation.

A. Through-transmission estimate of tissue attenuation

The ultrasonic attenuation slope of the *ex vivo* cervix sample was independently estimated by a double through-transmission insertion loss technique. The backscattered ultrasonic wave forms were recorded from a Plexiglas™ block placed at the focal plane both with and without the sealed cervix sample between the transducer and the block. With the sample present, ultrasound passed through the sample twice. The frequency-dependent attenuation of the cervix could then be determined by dividing the amplitude spectra and then fitting a line versus frequency to the log of the result after compensating for the passage of the ultrasound through the Saran Wrap. Compensating for the Saran Wrap was performed by measuring the thickness of the Saran Wrap using a micrometer and applying a correction term based on the density, sound speed, and thickness of the Saran Wrap as has been done previously (Madsen *et al.*, 1999). The spectra were obtained by scanning the ultrasound beam across 3 mm of the cervix tissue sample (step size ~15 μm) and averaging every 50 lines of the received spectra from the Plexiglas block. The scanning was performed using a Panametrics 5900™ pulser/receiver (Panametrics™, Waltham, MA) and a computer-controlled micropositioning system (Daedal, Inc., Harrisburg, PA). Each set of lines had 50% overlap with adjacent line sets so a total of seven measurements of attenuation were obtained for the cervix. An example of the normalized amplitude spectra from the Plexiglas block both with and without the cervix sample is shown in Fig. 3.

Likewise, an example of the estimated ultrasonic attenuation versus frequency after comparing the spectra is shown

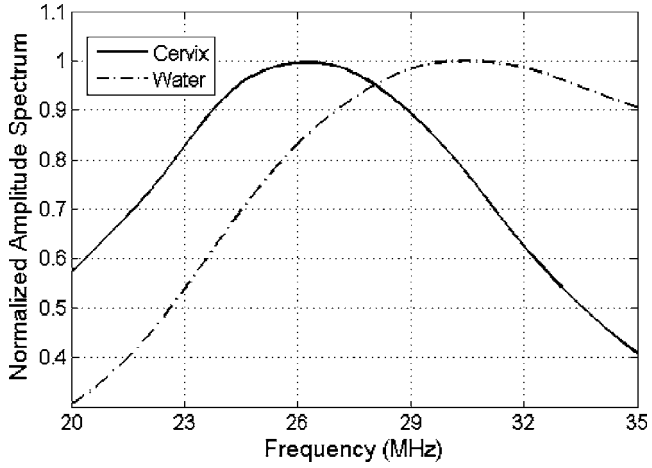

FIG. 3. An example of the normalized amplitude spectra from the Plexiglas block both with and without the cervix sample along the propagation path.

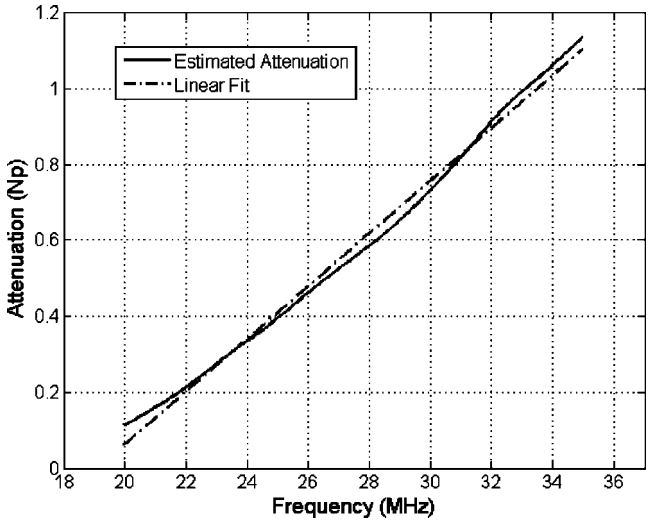

FIG. 4. An example of the estimated attenuation vs frequency after dividing the spectra shown with a linear fit vs frequency.

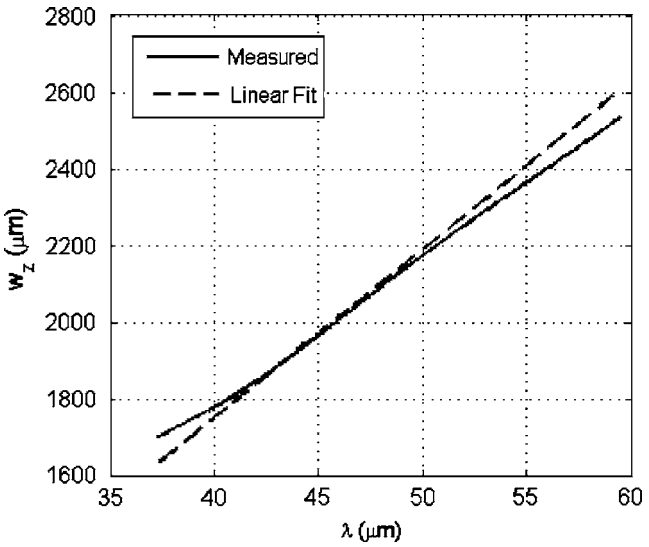

FIG. 5. Fitting a line through the measured w_z values to obtain an equation of w_z vs wavelength, λ.

in Fig. 4 along with a linear fit versus frequency. The equation for the linear fit to the attenuation values (in Np) for all seven measurements was $\alpha_{\text{true}}=(0.053\pm0.0098)f-1.25\pm0.068$ where f is in megahertz. Given that the thickness of the cervix was 1.86 ± 0.087 mm, this translates to an attenuation slope of 2.5 ± 0.4 dB/cm-MHz.

B. Determination of Gaussian depth of focus

Prior to implementing our algorithm using the *ex vivo* tissue sample, the Gaussian depth of focus, w_z, for the transducer needed to be determined as a function of wavelength. w_z was obtained for the transducer by obtaining echoes from a rigid plane located at different locations along the beam axis as controlled by a computer-controlled micropositioning system (Daedal, Inc., Harrisburg, PA) and fitting a Gaussian function versus depth to the reflected signal at each frequency. This gives a measurement of w_z at that frequency (Bigelow and O'Brien, 2004a, b). The results were generalized to other frequencies by fitting a line through the measured w_z values versus wavelength, λ, as shown in Fig. 5 for frequencies from 25 to 40 MHz. The fit was performed in terms of wavelength rather than frequency because we were anticipating a linear dependence on wavelength (Bigelow and O'Brien, 2004b). After performing the linear fit, we found that $w_z=43.8\lambda$ for the transducer used in the *ex vivo* experiment.

C. Pulse-echo estimate of attenuation using proposed algorithm

After measuring the attenuation of the cervix tissue sample by comparing the spectrum of the received signal from the Plexiglas block both with and without the tissue along the propagation path, the attenuation slope of the cervix tissue sample was estimated using our developed algorithm. The cervix tissue sample was positioned slightly in front of the focus (9 mm for this transducer) in a water bath and ultrasonic echoes from the cervix were obtained along a 3-mm length of the cervix using a step size of 15 μm. The scanning was performed using a Panametrics 5900 pulser/receiver and a computer-controlled micropositioning system (Daedal, Inc.). The echoes were windowed into five sections with each section having a depth of 0.48 mm. The sections overlapped by 50%, similar to the simulations, and spanned depths between 7.8 and 9.25 mm so that only echoes from within the cervix would be used in the estimate for attenuation. The echoes were then grouped into sets of 50 wave forms with 50% overlap between the sets and an estimate for $E[|V_{\text{refl}}(f)|]$ at each depth was obtained by averaging the amplitude spectrum of the 50 wave forms. The 50 wave forms spanned a range of approximately five beam widths, which was suggested to be optimal in terms of resolution versus estimate variance for parameters estimated from the frequency dependence of ultrasonic backscatter (Oelze and O'Brien, 2004). Then, prior to finding the frequency corresponding to the spectral peak at each depth, $E[|V_{\text{refl}}(f)|]$ was multiplied by $\exp(2z_0^2/w_z^2)$ using $w_z=43.8\lambda$ as was measured for our transducer while assuming a sound speed of water for the tissue.

The value for $\tilde{\sigma}_\omega$ and f_{peak} at each depth was then found by fitting the spectra to a Gaussian function using a frequency bandwidth of 40 MHz. Then, the value of $\tilde{\sigma}_\omega$ to be used in the calculation of attenuation slope was obtained by averaging the values of $\tilde{\sigma}_\omega$ obtained from the fit at each depth. Based on these calculations, the measured attenuation slope for the *ex vivo* tissue sample using our developed algorithm was 2.6 ± 0.6 dB/cm-MHz, which is in good agreement with the attenuation slope value of 2.5 ± 0.4 dB/cm-MHz using the basic insertion loss technique.

V. PRELIMINARY *IN VIVO* RESULTS

After completing the *ex vivo* experiment, the algorithm was used to obtain attenuation slope estimates for rat cervices *in vivo*. The experimental protocol was approved by the IACUC at the University of Illinois at Urbana-Champaign and satisfied all campus and NIH rules for the humane use of laboratory animals. Eight nonpregnant and 42 timed-pregnant (days 15, 17, 19, 20, and 21 of pregnancy) Sprague Dawley rats (Harlan) were randomly assigned to the *in vivo* experiment. After an adequate level of anesthesia was obtained [ketamine hydrochloride (87 mg/kg) and xylazine (13 mg/kg) administered intramuscularly], the rat was placed in dorsal recumbency and the ultrasonic transducer was inserted into the vaginal cavity of the rat with ultrasound coupling gel (Aquasonic 100, Parker Labs, Fairfield, NJ). The position of the transducer in the vagina was controlled by the computer-controlled micropositioning system (Daedal, Inc.). The backscattered signal from the cervix was then collected by a Panametrics 5900 pulser/receiver and monitored on an oscilloscope (Lecroy 9354 TM; Chestnut Ridge, NY). The position of the transducer was adjusted until the backscattered signal from the cervix was maximized.

Two different custom-fabricated 33-MHz lithium niobate ultrasonic transducers were used in the *in vivo* study because the original transducer used in the *ex vivo* experiment stopped working during the middle of the *in vivo* ex-

periments. The initial transducer had a focal length of 9.01 mm and a w_z value of $w_z=43.8\lambda$, while the second transducer had a focal length of 9.16 mm and a w_z value of $w_z=34.7\lambda+640$ μm. The value of w_z for the second transducer was found in the same manner as discussed in Sec. IV B. A total of 50 rats were used in the experiment including 8 nonpregnant rats, 8 rats at a gestational age of 15 days, 9 rats at a gestational age of 17 days, 8 rats at a gestational age of 19 days, 9 rats at a gestational age of 20 days, and 8 rats at a gestational age of 21 days.

After positioning, the transducer was scanned along the cervix using the micropositioning system (Daedal, Inc., Harrisburg, PA), and ultrasonic echoes were collected every 15 μm except for one scan of a nonpregnant rat where the echoes were collected every 10 μm. The usable scan width varied from 0.8 to 7 mm with a mean of 2.5 mm depending on the orientation of the cervix in the focal region and the animal's breathing. For 8 of the rats (2 at day 15, 1 at day 17, 3 at day 19, and 2 at day 21), no usable data were obtainable because the cervix was too far away from the focal region to correctly compensate for diffraction due to the bandwidth limitations of the transducer. Our method of compensating for diffraction by multiplying the spectrum by $\exp(2z_0^2/w_z^2)$ will amplify values of the spectrum at higher or lower frequencies depending on the value of z_0, the distance of the echo from the focus. Hence, for large values of z_0, the compensation term will only be amplifying noise and a reliable estimate for attenuation slope cannot be obtained.

After obtaining the usable echoes, the echoes were windowed into five sections with varying depths (0.33–0.9 mm with a mean of 0.56 mm) depending on the thickness of the cervix. The sections also overlapped in depth by 50%, similar to the simulations and *ex vivo* experiment. The echoes were then grouped into sets of 50 wave forms laterally with 50% overlap between adjacent sets and an estimate for $E[|V_{\mathrm{refl}}(f)|]$ at each depth was obtained by averaging the amplitude spectrum of the 50 wave forms. If a cervix had fewer than 50 usable wave forms, all of the wave forms were used to obtain an estimate. The number of attenuation slope estimates (i.e., sets of 50 wave forms) obtained for a particular cervix varied from 1 to 13 depending on the usable scan width for each cervix.

The attenuation slope estimates for all of the gestational ages are summarized in Fig. 6. The bars correspond to the mean attenuation slope value for a particular cervix at each gestational age while the error bars associated with each bar represent the standard deviation for that cervix. The horizontal lines and corresponding error bars associated with each gestational age are the means and standard deviations in cervix attenuation slope for all of the animals at a particular gestational age.

While it is challenging to compare the standard deviations due to the variable number of estimates obtained for each cervix, the variance in the mean cervix attenuation slope estimates between the animals at the same gestational age is larger than the variance between the different gestational ages. Also, the nonpregnant rats have a statistically significant ($p=0.029$) higher attenuation slope (3.2 ± 1.7 dB/cm-MHz) than the pregnant rats (mean over all gestational ages of 1.5 ± 1.3 dB/cm-MHz). However, a statistically significant effect of ultrasonic attenuation slope with gestational age is not observed because the variance in the estimates is too large.

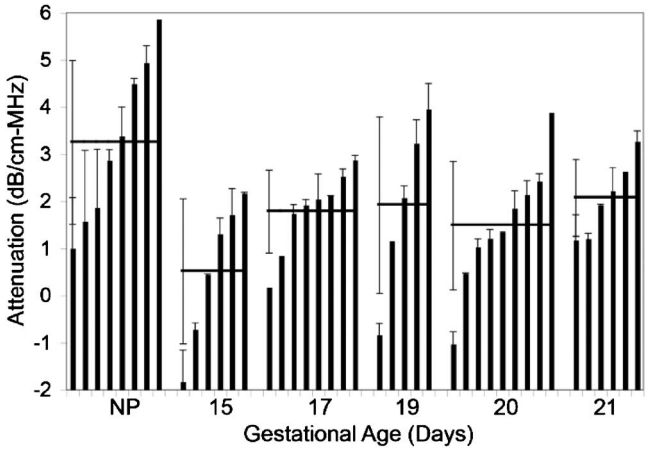

FIG. 6. *In vivo* ultrasound attenuation slope estimates for rat cervix showing the mean and standard deviation for every cervix sample (bars) vs gestational age as well as the mean and standard deviation for all of the cervices at each gestational age (horizontal lines).

VI. DISCUSSION

Our previous study suggested that cervical ripening and consequently preterm delivery could be predicted based on the ultrasonic attenuation of the cervix (McFarlin *et al.*, 2006). The goal of this study was to modify a traditional algorithm for estimating attenuation slope *in vivo*, so that it could be used to assess cervical ripening. The algorithm was modified by compensating for focusing by assuming the field along the beam axis in the focal region could be approximated by a Gaussian function and consequently multiplying the received spectra by an appropriate term. The validity of the modified algorithm was demonstrated via computer simulations and an *ex vivo* tissue experiment prior to being applied to *in vivo* experiments on rat cervices. In the simulations, the accuracy of the modified algorithm was better than 15%, and the attenuation slope of the cervix in the *ex vivo* experiment was found to be 2.6 ± 0.6 dB/cm-MHz, which is in good agreement with 2.5 ± 0.4 dB/cm-MHz estimated using an insertion loss technique.

For the *in vivo* experiments, the attenuation slope of the cervix for the nonpregnant rats was found to be approximately twice as much as the cervix for the pregnant rats on average (i.e., mean of 3.2 dB/cm-MHz versus mean of 1.5 dB/cm-MHz). However, the variance of the estimates was too large to deduce a statistically significant trend in the attenuation slope for the different gestational ages. The variance could probably be reduced by using a different animal model with a larger cervix so that more data could be used to estimate the amplitude spectrum of the backscattered signal. For example, the standard deviation for the attenuation slope for all of the rats at a gestational age of 20 days shown in Fig. 6 is 1.36 dB/cm-MHz. If we restrict our attention to only the three rats where more than 3 mm of the cervix could be scanned, the standard deviation between the different animals is 0.70 dB/cm-MHz.

The cause for the large variances is most likely the natural variation in attenuation for biological tissue between animals as is indicated by Fig. 6. Also, if we return to the three rats at a gestational age of 20 days where more than 3 mm of the cervix could be scanned, the standard deviation between the animals was 0.70 dB/cm-MHz, whereas the standard deviation for a particular animal was only 0.24 dB/cm-MHz on average. The variance in ultrasonic attenuation for tissue of the same type has been observed in other studies as well, e.g., glycogen in liver (Parker *et al.*, 1988; Tuthill *et al.*, 1989). Also, for example, many different attenuation coefficients for fat taken at different frequencies have been reported (Goss *et al.*, 1978). In particular, one study (Dussik and Fritch, 1956) gives attenuation values of 0.6 ± 0.2 dB/cm at 1 MHz and 2.3 ± 0.7 dB/cm at 5 MHz. Hence, for a change in frequency of 4 MHz, the change in attenuation varied from 0.8 to 2.6 dB/cm (i.e., 2.3−0.7 dB/cm minus 0.6+0.2 dB/cm and 2.3+0.7 dB/cm minus 0.6−0.2 dB/cm) yielding attenuation slopes between 0.2 and 0.65 dB/cm-MHz. Fortunately, the variance of an attenuation slope estimate of the cervix is manageable when considering a single animal with a sufficient number of backscattered echoes from the cervix. Therefore, longitudinal studies of attenuation slope estimates from individual rats throughout pregnancy are more likely to reveal statistically significant trends that could lead to prediction and detection of cervical ripening.

ACKNOWLEDGMENTS

This project was supported by Grant No. P30 NR009014 Center for Reducing Risks in Vulnerable Populations (CRRVP) from the National Institute of Nursing Research as well as the University of North Dakota School of Engineering and Mines. The project was also supported by Grant No. R01 CA111289. The content is solely the responsibility of the authors and does not necessarily represent the official views of the National Institute of Nursing Research or the National Institutes of Health.

Baldeweck, T., Herment, A., Laugier, P., and Berger, G. (**1994**). "Attenuation estimation in highly attenuating media using high frequencies: A comparison study between different mean frequency estimators," Proc.-IEEE Ultrason. Symp. **1783**, 1783–1786.

Baldeweck, T., Laugier, P., Herment, A., and Berger, G. (**1993**). "Application of autoregressive spectral analysis for ultrasound attenuation: Interest in highly attenuating medium," Proc.-IEEE Ultrason. Symp. **1182**, 1181–1186.

Baldeweck, T., Laugier, P., Herment, A., and Berger, G. (**1995**). "Application of autoregressive spectral analysis for ultrasound attenuation estimation: Interest in highly attenuating medium," IEEE Trans. Ultrason. Ferroelectr. Freq. Control **42**, 99–110.

Bigelow, T. A., and O'Brien, W. D., Jr. (**2004a**). "Scatterer size estimation in pulse-echo ultrasound using focused sources: Calibration measurements and phantom experiments," J. Acoust. Soc. Am. **116**, 594–602.

Bigelow, T. A., and O'Brien, W. D., Jr. (**2004b**). "Scatterer size estimation in pulse-echo ultrasound using focused sources: Theoretical approximations and simulation analysis," J. Acoust. Soc. Am. **116**, 578–593.

Callaghan, W. M., MacDorman, M. F., Rasmussen, S. A., Qin, C., and Lackritz, E. M. (**2006**). "The contribution of preterm birth to infant mortality rates in the United States," Pediatrics **118**, 1566–1573.

Clark, K., Ji, H., Feltovich, H., Janowski, J., Carroll, C., and Chien, E. K. (**2006**). "Mifepristone-induced cervical ripening: Structural, biomechanical, and molecular events," Am. J. Obstet. Gynecol. **194**, 1391–1398.

Dussik, K. T., and Fritch, D. J. (**1956**). "Determination of sound attenuation and sound velocity in the structure constituting the joints, and of the ultrasonic field distribution within the joints on living tissues and anatomical preparations, both in normal and pathological conditions," Public Health Service, National Institutes of Health Project No. A454, Progress Report, Washington, DC.

Feltovich, H., Ji, H., Janowski, J. W., Delance, N. C., Moran, C. C., and Chien, E. K. (**2005**). "Effects of selective and nonselective PGE2 receptor agonists on cervical tensile strength and collagen organization and microstructure in the pregnant rat at term," Am. J. Obstet. Gynecol. **192**, 753–760.

Girault, J. M., Ossant, F., Ouahabi, A., Kouame, D., and Patat, F. (**1998**). "Time-varying autoregressive spectral estimation for ultrasound attenuation in tissue characterization," IEEE Trans. Ultrason. Ferroelectr. Freq. Control **45**, 650–659.

Goss, S. A., Johnston, R. L., and Dunn, F. (**1978**). "Comprehensive compilation of empirical ultrasonic properties of mammalian tissues," J. Acoust. Soc. Am. **64**, 423–457.

Hamilton, B. E., Martin, J. A., and Ventura, S. J. (**2006**). "Births: Preliminary data for 2005," Natl. Vital Stat. Rep. **55**, 1–18.

House, M., and Socrate, S. (**2006**). "The cervix as a biomechanical structure," Ultrasound Obstet. Gynecol. **28**, 745–749.

Hyungsuk, K., and Varghese, T. (**2007**). "Attenuation estimation using spectral cross-correlation," IEEE Trans. Ultrason. Ferroelectr. Freq. Control **54**, 510–519.

Insana, M. F., Wagner, R. F., Brown, D. G., and Hall, T. J. (**1990**). "Describing small-scale structure in random media using pulse-echo ultrasound," J. Acoust. Soc. Am. **87**, 179–192.

Leppert, P. C. (**1995**). "Anatomy and physiology of cervical ripening," Clin. Obstet. Gynecol. **38**, 267–279.

Leppert, P. C., Kokenyesi, R., Klemenich, C. A., and Fisher, J. (**2000**). "Further evidence of a decorin-collagen interaction in the disruption of cervical collagen fibers during rat gestation," Am. J. Obstet. Gynecol. **182**, 805–812.

Madsen, E. L., Dong, F., Frank, G. R., Garra, B. S., Wear, K. A., Wilson, T., Zagzebski, J. A., Miller, H. L., Shung, K. K., Wang, S. H., Feleppa, E. J., Liu, T., O'Brien, W. D., Jr., Topp, K. A., Sanghvi, N. T., Zaitsev, A. V., Hall, T. J., Fowlkes, J. B., Kripfgans, O. D., and Miller, J. G. (**1999**). "Interlaboratory comparison of ultrasonic backscatter, attenuation, and speed measurements," J. Ultrasound Med. **18**, 615–631.

Mahendroo, M. S., Porter, A., Russell, D. W., and Word, R. A. (**1999**). "The parturition defect steroid 5{alpha}-reductase type 1 knockout mice is due to impaired cervical ripening," Mol. Endocrinol. **13**, 981–992.

McFarlin, B. L., O'Brien, W. D., Jr., Oelze, M. L., Zachary, J. F., and White-Traut, R. C. (**2006**). "Quantitative ultrasound assessment of the rat cervix," J. Ultrasound Med. **25**, 1031–1040.

Narayana, P. A., and Ophir, J. (**1983a**). "A closed form method for the measurement of attenuation in nonlinearly dispersive media," Ultrason. Imaging **5**, 17–21.

Narayana, P. A., and Ophir, J. (**1983b**). "On the validity of the linear approximation in the parametric measurement of attenuation in tissues," Ultrasound Med. Biol. **9**, 357–361.

Oelze, M. L., and O'Brien, W. D., Jr. (**2004**). "Defining optimal axial and lateral resolution for estimating scatterer properties from volumes using ultrasound backscatter," J. Acoust. Soc. Am. **115**, 3226–3234.

Oosterveld, B. J., Thijssen, J. M., Hartman, P. C., Romijn, R. L., and Rosenbusch, G. J. E. (**1991**). "Ultrasound attenuation and texture analysis of diffuse liver disease: Methods and preliminary results," Phys. Med. Biol. **36**, 1039–1064.

Parker, K. J., Tuthill, T. A., and Baggs, R. B. (**1988**). "The role of glycogen and phosphate in ultrasonic attenuation of liver," J. Acoust. Soc. Am. **83**, 374–378.

St. John, E. B, Nelson, K. G., Cliver, S. P., Bishnoi, R. R., and Goldenberg, R. L. (**2000**). "Cost of neonatal care according to gestational age at birth and survival status," Am. J. Obstet. Gynecol. **182**, 170–175.

Straach, K. J., Shelton, J. M., Richardson, J. A., Hascall, V. C., and Mahendroo, M. S. (**2005**). "Regulation of hyaluronan expression during cervical ripening," Glycobiology **15**, 55–65.

Tuthill, T. A., Baggs, R. B., and and Parker, K. J. (**1989**). "Liver glycogen and water storage: Effect on ultrasound attenuation," Ultrasound Med. Biol. **15**, 621–627.

Wilson-Costello, D., Friedman, H., Minich, N., Siner, B., Taylor, G., Schluchter, M., and Hack, M. (**2007**). "Improved neurodevelopmental outcomes for extremely low birth weight infants in 2000-2002," Pediatrics **119**, 37–45.